Title	Reduction of channel coupling effect on Li isotope elastic scatterings by glue-like behaviour of excess neutron
Author(s)	Furumoto, Takenori; Suhara, Tadahiro; Itagaki, Naoyuki
Citation	AIP Conference Proceedings (2018), 2038(1)
Issue Date	2018-11-13
URL	http://hdl.handle.net/2433/254189
Right	This article may be downloaded for personal use only. Any other use requires prior permission of the author and AIP Publishing. This article appeared in (citation of published article) and may be found at https://doi.org/10.1063/1.5078858
Type	Journal Article
Textversion	publisher

Reduction of channel coupling effect on Li isotope elastic scatterings by glue-like behaviour of excess neutron

Cite as: AIP Conference Proceedings **2038**, 020039 (2018); https://doi.org/10.1063/1.5078858
Published Online: 13 November 2018

Takenori Furumoto, Tadahiro Suhara, and Naoyuki Itagaki

Reduction of channel coupling effect on Li isotope elastic scatterings by glue-like behaviour of excess neutron

Takenori Furumoto[1,a)], Tadahiro Suhara[2,b)] and Naoyuki Itagaki[3,c)]

[1]*Graduate School of Education, Yokohama National University, Yokohama 240-8501, Japan*
[2]*Matsue College of Technology, Matsue, Shimane 690-8518, Japan*
[3]*Yukawa Institute for Theoretical Physics, Kyoto University, Kyoto 606-8502, Japan*

[a)]Corresponding author: furumoto-takenori-py@ynu.ac.jp
[b)]suhara@matsue-ct.ac.jp
[c)]itagaki@yukawa.kyoto-u.ac.jp

Abstract. The glue-like behavior of valence neutrons has been investigated in the Li isotopes. The ^{7}Li nucleus is well known to be weakly bound system with the $\alpha + t$ cluster structure. By adding the valence neutrons, the reduction of the root-mean-square (RMS) radius of the proton density for the ^{7}Li, ^{8}Li and, ^{9}Li nuclei is also well known from the viewpoint of the experimental data and theoretical approach. Elastic scattering cross sections of the Li isotopes on the ^{12}C and ^{28}Si targets at $E/A \sim 50$ MeV are calculated. We find the change of the channel coupling (CC) effect on elastic scatterings of such Li isotopes by the glue-like role of the valence neutrons. Finally, we realize that the valence neutrons stabilize the binding of core parts, and the CC effect related the core excitation is indeed reduced.

INTRODUCTION

The glue-like behavior of neutrons is one of hot topics in nuclear cluster physics field. The ^{8}Be ($\alpha+\alpha$) nucleus is well known as an unbound system. The ^{9}Be ($\alpha+\alpha+n$) nucleus is bound by the addition of a neutron. The valence neutrons play various roles in the ^{10}Be and ^{12}Be nuclei in the ground and excited states [1, 2, 3]. Furthermore, the valence neutrons show the glue-like role in the ^{14}C nucleus to stabilize the three-α-cluster states, including the linear-chain configurations [4, 5]. However, it is difficult to compare the ^{8}Be and ^{9}Be nuclei directly from the viewpoint of the nuclear reaction. Because ^{8}Be is unbound system.

Therefore, we focus on Li isotopes which have an analog structure of Be isotopes. The Li isotopes are considered as replacing an α cluster in Be isotopes by a t cluster. In addition, the ^{7}Li nucleus is bound system as contrasted with the ^{8}Be nucleus. Namely, the observation of Li isotopes is a good motivation to investigate the glue-like role. Historically, the ^{6}Li and ^{7}Li nuclei, which are well known as α+d (α+p+n) and α+t cluster systems, respectively, are investigated. The breakup effects of the ^{6}Li and ^{7}Li nuclei into α+d (α+p+n) and α+t systems, respectively, contribute to elastic scattering cross section strongly [6, 7, 8]. In this paper, we analyze the elastic scattering of the Li isotopes including ^{8}Li and ^{9}Li nuclei to reveal the role of their valence neutrons.

In order to investigate the role of valence neutrons in ^{8}Li and ^{9}Li nuclei, we apply the microscopic nuclear structure and reaction calculations. First, Li isotopes are constructed by the stochastic multi-configuration mixing (SMCM) method based on the cluster model. The SMCM method has been known to well describe the structure of light nuclei, not only for the ground state but also for the excited state [9, 10]. Next, the elastic scattering of Li isotopes is described by the microscopic coupled-channel (MCC) method based on the folding procedure with the complex G-matrix interaction. The folding model with the complex G-matrix interaction well works to reproduce the heavy-ion scatterings [11, 12, 13, 14, 15].

In this paper, we check the ^{6}Li, ^{7}Li, ^{8}Li, and ^{9}Li nuclei constructed by the SMCM calculation for the excitation energies, root-mean-square (RMS) radii of nucleon densities, transition strengths (B($IS2$)). Next, the elastic scattering cross sections of the ^{6}Li and ^{7}Li nuclei on the ^{12}C and ^{28}Si targets at $E/A \sim 50$ MeV are firstly compared with the experimental data. After that, we find the change of the channel coupling (CC) effect on elastic scatterings of ^{7}Li, ^{8}Li,

Proceedings of the 4th International Workshop on "State of the Art in Nuclear Cluster Physics" (SOTANCP4)
AIP Conf. Proc. 2038, 020039-1–020039-6; https://doi.org/10.1063/1.5078858
Published by AIP Publishing. 978-0-7354-1764-9/$30.00

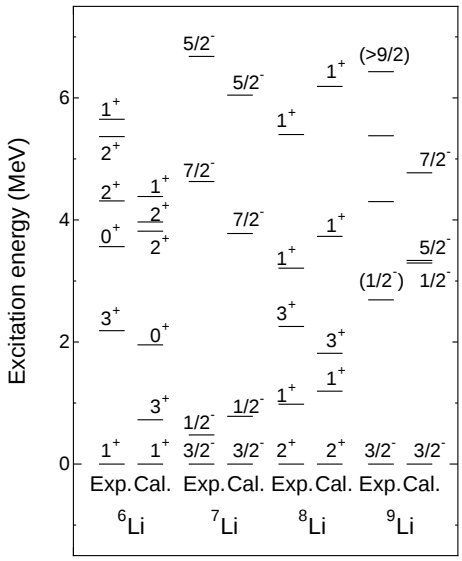

FIGURE 1. Excitation energy of the experimental data and calculated results of the Li isotopes. The experimental data are taken from Ref. [18].

and ^{9}Li nuclei by the glue-like role of the valence neutrons. Finally, we realize that the valence neutrons stabilize the binding of core parts, and the CC effect related the core excitation is indeed reduced.

FORMALISM

Our model is based on the microscopic calculations for nuclear structure and reaction. The wave functions of the Li isotopes are obtained by the SMCM method based on the cluster models. For ^{6}Li, ^{7}Li, and ^{9}Li, the $\alpha + p + n$, $\alpha + p + n + n$ and $\alpha + t + n + n$ cluster models are applied, respectively. For ^{8}Li, the $\alpha + t + n$ and $\alpha + p + n + n + n$ cluster configurations are mixed. After nuclear structure calculations, we apply the wave functions to the microscopic coupled-channel (MCC) method based on the folding procedure with the complex G-matrix interaction. The more detailed method is introduced in Refs. [16, 17].

RESULT

Energies, RMS radii, and transition strengths

Here, we summarize the results of the structure calculation with the SMCM method. Figure 1 shows low-lying excitation energies for the ^{6}Li, ^{7}Li, ^{8}Li, and ^{9}Li nuclei corresponded to the experimental data. The more detailed values of the excitation energies are shown in Ref. [17]. The calculated results well reproduce the experimental data.

Table 1 shows the calculated RMS radii of the charged proton, point proton, point neutron and point matter densities. The theoretical RMS radius of the charged proton density is obtained by folding the point proton density distribution with the proton charge form factor. The calculated RMS radii of the point neutron and point matter densities well reproduce the experimental data. The trend of the decrease in the proton radius exhibits the glue-like behavior of the valence neutrons, which attract the α–t clusters in the Li isotopes.

Table 2 shows the calculated transition strengths (B($IS2$)) from the ground states to the excited states but for B($IS2$) > 10 fm^4. When we see the ^{7}Li and ^{9}Li nuclei, the transition strength between states of the same angular momenta is found to have certainly decreased. The decreased transition strength of the ^{9}Li nucleus is considered to be contributed by the glue-like role of valence neutrons. By attracting the α and t clusters, the ^{9}Li nucleus gives the small radius and consistently results of a small transition strength in the comparison with the ^{7}Li nucleus.

TABLE 1. RMS radii of the charged proton [point proton], point neutron and point matter densities for the ground states of the ^{6}Li, ^{7}Li, ^{8}Li, and ^{9}Li nuclei.

	Charged proton (fm)	Point neutron (fm)	Point matter (fm)
Cal.	[Point proton]		
^{6}Li	2.662 [2.523]	2.556	2.539
^{7}Li	2.636 [2.495]	2.604	2.558
^{8}Li	2.530 [2.379]	2.615	2.529
^{9}Li	2.393 [2.237]	2.562	2.445
Exp. [19]			
^{6}Li	2.54(3)	2.54(3)	2.54(3)
^{7}Li	2.43(3)	2.54(3)	2.50(3)
^{8}Li	2.41(3)	2.57(3)	2.51(3)
^{9}Li	2.30(2)	2.50(2)	2.43(3)
Exp. [20]			
^{6}Li	2.517(30)		
^{8}Li	2.299(32)		
^{9}Li	2.217(35)		

TABLE 2. Transition strengths $B(IS2)$ from the ground states to the excited states for the ^{6}Li, ^{7}Li, ^{8}Li, and ^{9}Li nuclei.

^{6}Li	B($IS2$) (fm^4)	^{7}Li	B($IS2$) (fm^4)	^{8}Li	B($IS2$) (fm^4)	^{9}Li	B($IS2$) (fm^4)
3^+_1	57.13	$1/2^-_1$	54.47	1^+_1	16.24	$1/2^-_1$	19.26
2^+_1	54.78	$7/2^-_1$	96.78	3^+_1	47.94	$5/2^-_1$	19.19
1^+_2	33.56	$5/2^-_1$	22.06	2^+_3	15.68	$7/2^-_1$	31.55

Elastic scattering of Li isotopes

Next, we show the results of the MCC calculation. The elastic-scattering cross sections for the ^{12}C and ^{28}Si targets using the transition densities are obtained. The imaginary part of the diagonal and transition potentials obtained by the folding procedure is multiplied by a renormalization factor, N_W, as follows:

$$U = V + iN_{\rm W}W, \tag{1}$$

where, V and W represent the real and imaginary parts of the folding model potentials, respectively. $N_{\rm W}$ is the only free parameter in the present calculation.

The transition densities of the target nuclei (^{12}C and ^{28}Si) were obtained in the following manner. For the ^{12}C target, the transition density is taken from Ref. [21]. For the ^{28}Si target, we apply the nucleon densities to be deduced from the charge densities [22] extracted from the electron-scattering experiments by unfolding the charge form factor of a proton in the standard way [23]. In addition, we apply the Bohr-Mottelson-type collective model [24] and a relation based on the $K = 0$ rotational band [25] to construct the quadrupole ($\lambda = 2$) components of the transition density in a manner same as Ref. [26]. The more information of the contributed excited states is introduced in Ref. [17].

Here we note that the calculated results including the excitation effects of both projectile and target nuclei are referred to as "full-CC". The calculated results include no excitation effects were referred to as "1-ch". The results for "^{12}C* only" and "^{28}Si* only" include only the target excitation effect.

Comparison of calculated results with experimental data

In this section, we test the present SMCM method with the experimental data using the MCC calculation for light heavy-ion elastic scatterings. Figure 2 shows the ^{6}Li elastic scatterings by the ^{12}C and ^{28}Si targets at $E/A = 53$ MeV. The experimental data are well reproduced up to backward angles with $N_W = 0.7$. The CC effects on the elastic cross section of the ^{6}Li, ^{12}C, and ^{28}Si nuclei are clearly seen. The ^{6}Li and ^{12}C (^{28}Si) nuclei give comparable CC effects in the ^{6}Li + ^{12}C (^{28}Si) elastic scattering.

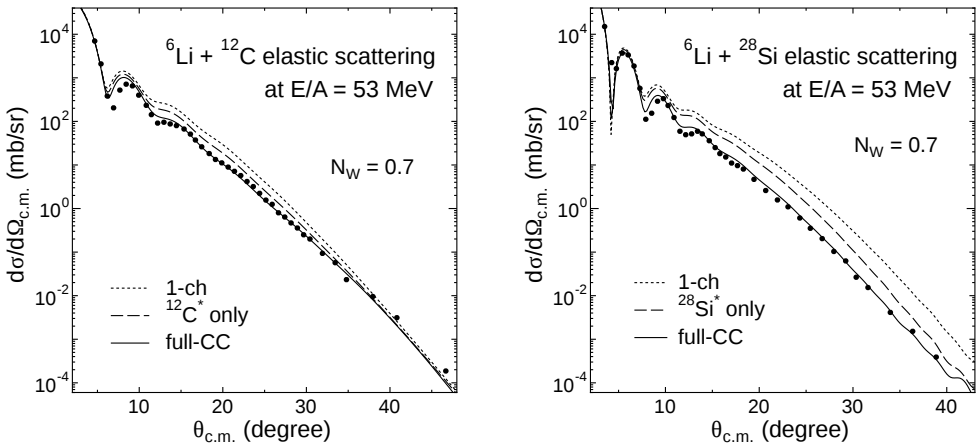

FIGURE 2. Elastic cross section for the ^{6}Li + ^{12}C and ^{6}Li + ^{28}Si systems at E/A = 53 MeV. The experimental data are taken from Ref. [27].

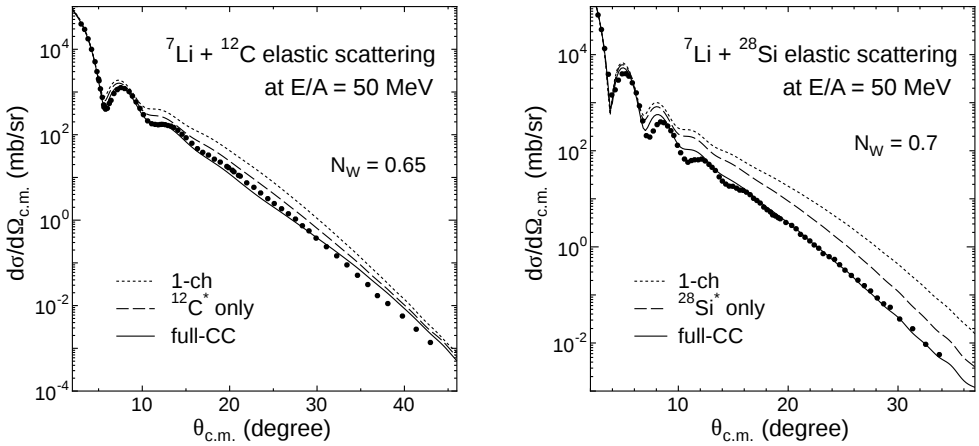

FIGURE 3. Elastic cross section for the ^{7}Li + ^{12}C and ^{7}Li + ^{28}Si systems at E/A = 50 MeV. The experimental data are taken from Ref. [28].

Figure 3 shows ^{7}Li elastic scatterings by the ^{12}C and ^{28}Si targets at E/A = 50 MeV. We see good reproduction of the experimental data with N_W = 0.65 and 0.7. In addition, the CC effects on the elastic cross section of the ^{7}Li, ^{12}C, and ^{28}Si nuclei are clearly seen. Again, the ^{6}Li and ^{12}C (^{28}Si) nuclei give comparable CC effects in the ^{6}Li + ^{12}C (^{28}Si) elastic scattering.

Demonstration of CC effect by ^{7}Li, ^{8}Li, and ^{9}Li nuclei

In the previous section, we see good reproduction of the experimental data for ^{6}Li and ^{7}Li elastic scatterings when the renormalization factor is adjusted to around 0.7. Here, we fix the renormalization factor to be 0.7 to demonstrate the elastic cross section of the Li isotopes. Note that our conclusions remain unchanged even if we take another value near N_W = 0.7.

Figure 4 shows ^{7}Li, ^{8}Li, and ^{9}Li elastic scatterings by the ^{12}C and ^{28}Si targets at E/A = 53 MeV. We first find that the CC effects by both the projectile and target nuclei work almost comparably for ^{7}Li + ^{12}C and ^{7}Li + ^{28}Si elastic scatterings. On the other hand, a smaller CC effect by the ^{8}Li and ^{9}Li nuclei can be seen in the comparison with the target nuclei in Fig. 4. This change implies that the valence neutrons behave an important glue-like role to attract the α and t clusters in the ^{8}Li and ^{9}Li nuclei. By the glue-like role of the valence neutrons, the RMS radii of the proton densities for the ^{8}Li and ^{9}Li nuclei become smaller. The shrinkage of the ^{8}Li and ^{9}Li nuclei gives a small transition strength. The reduction of the CC effect by the ^{8}Li and ^{9}Li nuclei is obtained by decreasing transition strength in the

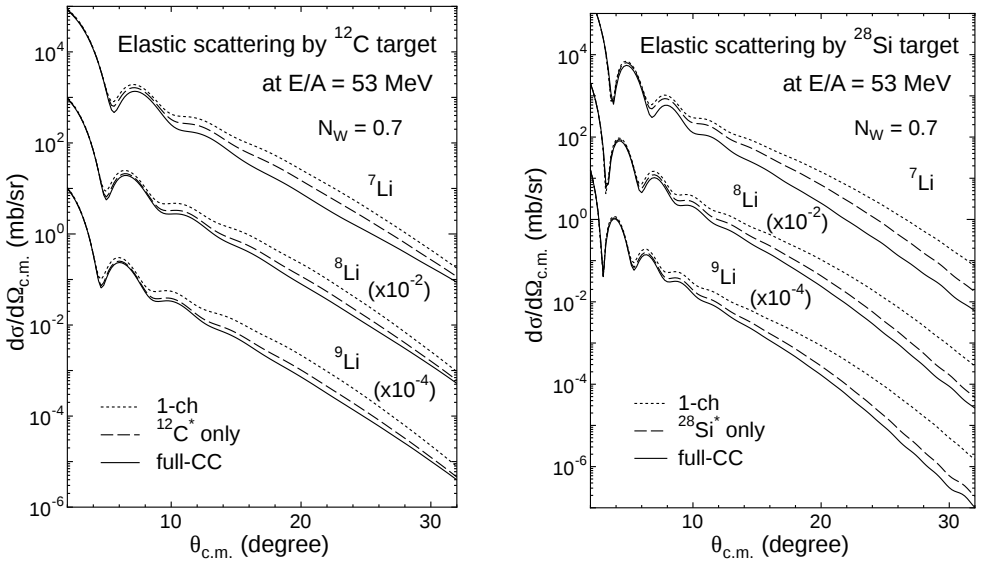

FIGURE 4. Elastic scattering of the ^{7}Li, ^{8}Li, and ^{9}Li nuclei for the ^{12}C and ^{28}Si targets at $E/A = 53$ MeV.

comparison with the ^{7}Li elastic scattering. In the neutron-rich nuclei, we roughly expected that the CC effect will be important since the particle-decay thresholds were always low. This may be true for the fact that the continuum states for the valence neutrons made significant contribution; however, the valence neutrons also exhibit an aspect of stabilizing the binding of core parts. Therefore, the CC effect relates to core excitation is indeed reduced when we perform a direct comparison with the case involving weakly bound core nuclei.

Summary

We apply the microscopic frameworks for structure and reaction to investigate the channel coupling (CC) effect on the elastic scatterings of the Li isotopes (A = 6–9) for the ^{12}C and ^{28}Si targets at $E/A \sim 50$ MeV. The wave functions of the Li isotopes are obtained with the stochastic multi-configuration mixing (SMCM) method based on the microscopic cluster model, which yields reasonable results for the excitation energies and radii in comparison with the experimental data. The RMS radii of the proton density for the ^{7}Li, ^{8}Li, and ^{9}Li nuclei become smaller with increasing valence neutron additions. A comparison of the ^{7}Li and ^{9}Li nuclei shows that the transition strength, B(IS2), also become smaller because of the addition of valence neutrons. This implies that the valence neutrons have an important glue-like behavior. Namely, they are found to bind the $\alpha + t$ clusters in the Li isotopes.

The elastic scatterings of the Li isotopes are obtained in the framework of the microscopic coupled-channel (MCC) method with the results of the SMCM calculation. The existing experimental data are well reproduced for ^{6}Li and ^{7}Li elastic scatterings by the ^{12}C and ^{28}Si targets at E/A = 50 and 53 MeV, respectively. In addition, the CC effects of the projectile and target nuclei are clearly seen on the elastic cross sections. The ^{7}Li, ^{8}Li, and ^{9}Li elastic cross sections are demonstrated for the ^{12}C and ^{28}Si targets at E/A = 53 MeV with the excitation effects of the projectile and target nuclei. The ^{8}Li and ^{9}Li nuclei give the reduction of the CC effects in comparison with the ^{7}Li nucleus, which is thought to be caused by the glue-like behavior exhibited by the valence neutrons; the α–t core is stabilized by adding neutrons. We find that the glue-like role of the valence neutrons in the Li isotopes contributes not only to the RMS radii and the transition strengths but also to the CC effect on the elastic cross sections. In the neutron-rich nuclei, we roughly expect that the CC effect will be important since the particle-decay thresholds were always low. This could possibly be true for the fact that the continuum states for valence neutrons made significant contribution; however, the valence neutrons also tend to stabilize the binding of core parts. Therefore, the CC effect due to the core excitation is indeed reduced when we perform a direct comparison of this case with the case involving weakly bound core nuclei.

ACKNOWLEDGMENTS

This work was supported by the Japan Society for the Promotion of Science (JSPS) KAKENHI Grants No. JP15K17661, No. JP15K17662, and No. JP17K05440.

REFERENCES

[1] N. Itagaki and S. Okabe, Phys. Rev. C **61**, p. 044306 (2000).
[2] M. Ito, N. Itagaki, H. Sakurai, and K. Ikeda, Phys. Rev. Lett. **100**, p. 182502 (2008).
[3] M. Kimura, T. Suhara, and Y. Kanada-En'yo, Eur. Phys. J. **A52**, p. 373 (2016).
[4] N. Itagaki, T. Otsuka, K. Ikeda, and S. Okabe, Phys. Rev. Lett. **92**, p. 142501 (2004).
[5] T. Suhara and Y. Kanada-En'yo, Phys. Rev. C **82**, p. 044301 (2010).
[6] Y. Sakuragi, M. Yahiro, and M. Kamimura, Prog. Theor. Phys. Suppl. **89**, p. 136 (1986).
[7] Y. Sakuragi, Phys. Rev. C **35**, p. 2161 (1987).
[8] S. Watanabe, T. Matsumoto, K. Ogata, and M. Yahiro, Phys. Rev. C **92**, p. 044611 (2015).
[9] T. Ichikawa, N. Itagaki, T. Kawabata, T. Kokalova, and W. von Oertzen, Phys. Rev. C **83**, p. 061301(R) (2011).
[10] K. Muta, T. Furumoto, T. Ichikawa, and N. Itagaki, Phys. Rev. C **84**, p. 034305 (2011).
[11] T. Furumoto, Y. Sakuragi, and Y. Yamamoto, Phys. Rev. C **80**, p. 044614 (2009).
[12] T. Furumoto, W. Horiuchi, M. Takashina, Y. Yamamoto, and Y. Sakuragi, Phys. Rev. C **85**, p. 044607 (2012).
[13] Y. Yamamoto, T. Furumoto, N. Yasutake, and T. A. Rijken, Phys. Rev. C **90**, p. 045805 (2014).
[14] T. Furumoto, Y. Sakuragi, and Y. Yamamoto, Phys. Rev. C **94**, p. 044620 (2016).
[15] W. W. Qu, G. L. Zhang, S. Terashima, T. Furumoto, Y. Ayyad, Z. Q. Chen, C. L. Guo, A. Inoue, X. Y. Le, H. J. Ong, D. Y. Pang, H. Sakaguchi, Y. Sakuragi, B. H. Sun, A. Tamii, I. Tanihata, T. F. Wang, R. Wada, and Y. Yamamoto, Phys. Rev. C **95**, p. 044616 (2017).
[16] T. Furumoto, T. Suhara, and N. Itagaki, Phys. Rev. C **87**, p. 064320 (2013).
[17] T. Furumoto, T. Suhara, and N. Itagaki, Phys. Rev. C **97**, p. 044602 (2018).
[18] http://www.nndc.bnl.gov/ ().
[19] I. Tanihata, H. Hamagaki, O. Hashimoto, Y. Shida, N. Yoshikawa, K. Sugimoto, O. Yamakawa, T. Kobayashi, and N. Takahashi, Phys. Rev. Lett. **55**, p. 2676 (1985).
[20] R. Sánchez, W. Nörtershäuser, G. Ewald, D. Albers, J. Behr, P. Bricault, B. Bushaw, A. Dax, J. Dilling, M. Dombsky, G. Drake, S. Götte, R. Kirchner, H.-J. Kluge, T. Kühl, J. Lassen, C. Levy, M. Pearson, E. Prime, V. Ryjkov, A. Wojtaszek, Z.-C. Yan, and C. Zimmermann, Phys. Rev. Lett. **96**, p. 033002 (2006).
[21] M. Kamimura, Nucl. Phys. **A351**, p. 456 (1981).
[22] H. DeVries, C. W. DeJager, and C. DeVries, At. Data Nucl. Data Tables **36**, p. 495 (1987).
[23] L. R. B. Elton, *Nuclear Size* (Oxford University, Oxford, 1961).
[24] G. R. Satchler, *Direct Nuclear Reactions* (Oxford University, Oxford, 1983).
[25] A. Bohr and B. R. Mottelson, *Nuclear Structure* (World Scientific, Singapore City, 1975).
[26] D. T. Khoa and G. R. Satchler, Nucl. Phys. **A668**, p. 3 (2000).
[27] A. Nadasen, T. Stevens, J. Farhat, J. Brusoe, P. Schwandt, J. Winfield, G. Yoo, N. Anantaraman, F. Becchetti, J. Brown, B. Hotz, J. Jänecke, D. Roberts, and R. E. Warner, Phys. Rev. C **47**, p. 674 (1993).
[28] A. Nadasen, J. Brusoe, J. Farhat, T. Stevens, J. Williams, L. Nieman, J. Winfield, R. Warner, F. Becchetti, J. Jänecke, T. Annakkage, J. Bajema, D. Roberts, and H. Govinden, Phys. Rev. C **52**, p. 1894 (1995).